Electronic Supplementary Material (ESI) for Energy & Environmental Science.

Supplemental information

1. Working principles of CVD and ALD techniques

In CVD, a solid material is produced from a vapor precursor via a chemical reaction. Such a reaction may take place either on a surface or in a gas phase. Typically, two types of reactions are distinguished in CVD: (i) thermal (pyrolytic) decomposition and (ii) exchange reaction. In both cases, the gaseous reactant(s) is continuously admitted into the reactor by the flow of a gaseous precursor and the gaseous by product(s) is continuously removed out of it. However, the former associates with the decomposition of single gaseous reactant whereas the latter relies on the reaction between two gaseous reactants. And the solid material that nucleated on the surface of substrate is obtained in the form of a coating, powder, or single crystal. **Figure S1** illustrates such reactions for a thin film growth.

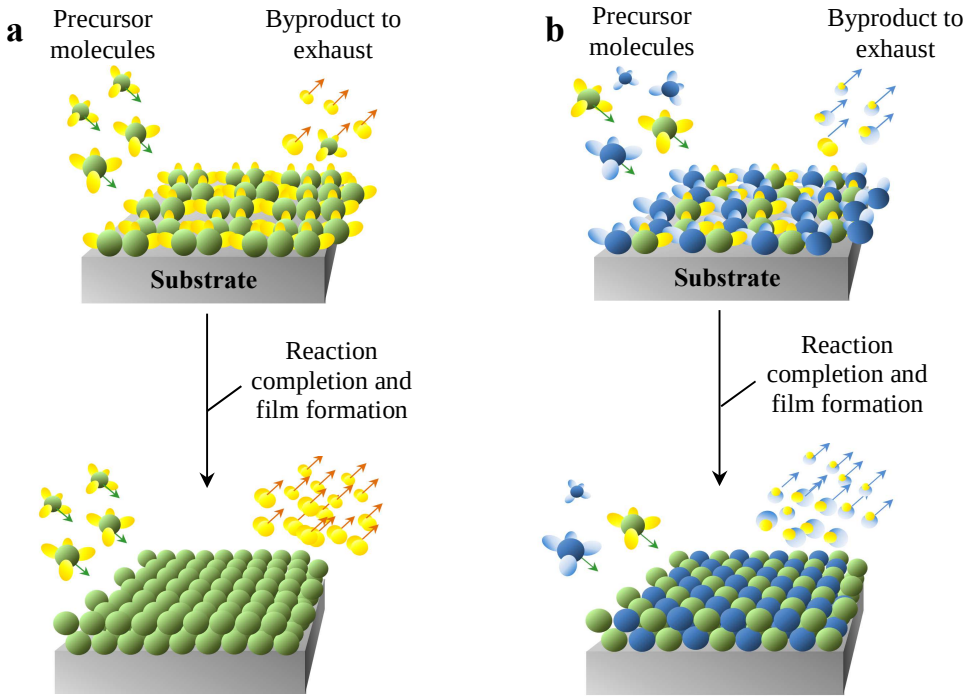

Figure S1. Simplified schematic of the two most common types of thin film deposition by CVD: (a) thermal decomposition (pyrolytic) reaction and (b) exchange reaction. In both cases the precursor molecules are continuously supplied and the gaseous byproduct molecules are continuously removed. Reaction conditions need to be tuned in order to avoid chemical reaction in a gaseous phase, which may lead to surface roughening and formation of nanoparticles.

ALD is a surface-controlled process that applies a strategy of sequential exposure and purge steps to remove all the physisorbed molecule(s) from the system **(Figure S2)**. In contrast to CVD, the gaseous precursors are supplied one at a time into the reactor and purge steps are applied between reactant introductions. In a typical ALD cycle, a first gaseous precursor introduced into the system forms a chemically-bonded molecule layer on the substrate surface with all the physisorbed (extra) molecules cleaned off by the following purging process. When a second precursor vapor is introduced, it reacts selectively with the chemisorbed layer of the first precursor, thus creating a monomolecular-level layer of an ALD coating. The excess (physisorbed) molecules of the second precursors are similarly purged off with an inert gas. By repeating the process cycles, atomic layer-by-layer growth of the coating is achieved with a precise control over the thickness governed by the number of ALD cycles. Benefitting from such a precise operation where only chemically-bonded molecule(s) can react on the surface for each exposure, ALD could give rise to very dense, conformal[1], uniform and very thin (sub-nm, if needed) coatings on complex 3D porous substrates. Another advantage of ALD - it generally requires lower reaction temperature than CVD. While plasma enhancement reduces deposition temperature for both processes, plasma-assisted ALD (PA-ALD) allows deposition at room temperature and even below, which could be particularly attractive for coating deposition on thermally sensitive substrates. The serious limitation of ALD, in turn, is a relatively slow deposition rate.

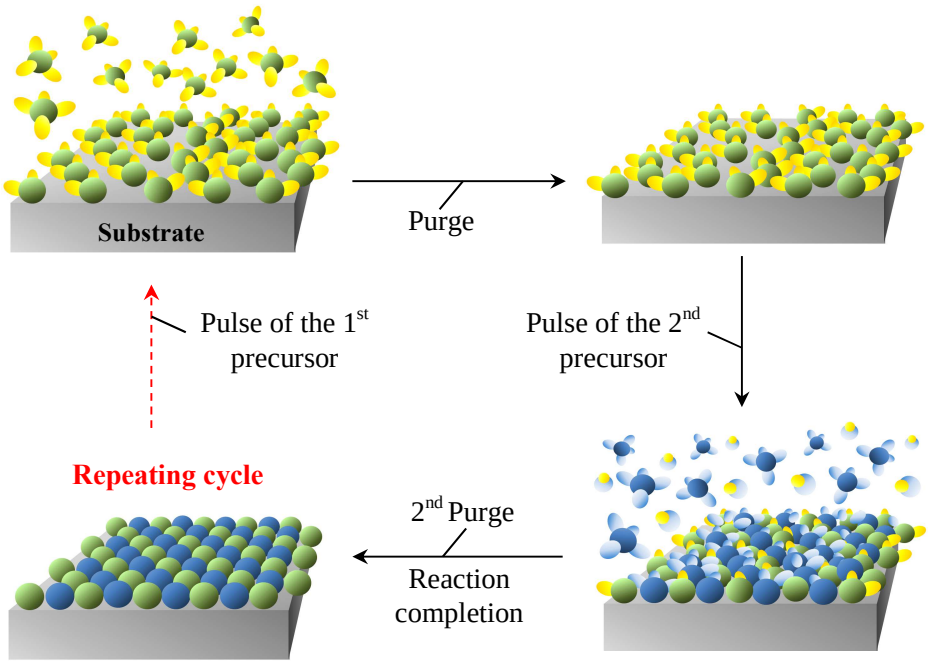

Figure S2. Simplified schematic of thin film formation by ALD. The precursors are introduced one at a time with a purge cycle in between. The reaction occurs only on the surface and very uniform film formation on porous substrates becomes possible.

2. Mechanism of CVD growth of nanowire

A CVD growth of various nanostructures on substrates will be illustrated using nanowire growth as the most general example (**Figure S3**). Their growth commonly follows the so-called vapor-liquid-solid (VLS) mechanism.[2] Three growth types could be distinguished: the tip (floating) catalyst growth, root catalyst growth and catalyst-free (self-catalytic) growth (**Figure S3a**).In the case of a tip catalyst growth, the catalyst-substrate interaction is weak (catalyst has an acute contact angle with the substrate), the gaseous precursor decomposes on the surface of a catalyst and (in a most common case of a liquid catalyst) the precursor species (e.g., individual atoms) dissolve into it. Due to the concentration gradient, the precursor diffuses down through the catalyst. After reaching saturation or supersaturation (at a fixed growth temperature), the as-dissolved precursor precipitates out and nucleates at the liquid/solid interphase, leading to an axial crystal growth and pushing the catalyst droplet off the substrate. Three types of catalysts could be distinguished: (i) all-liquid catalyst seed (**FigureS3b**, left),[2] where precursor species diffuse through the bulk of the catalyst; (ii) solid catalyst with the liquid layer at the surface and at the interface with the nanowire,(Figure S3b, middle),[3, 4] where precursors diffuse along the

surface to the liquid-solid interface before being incorporated into the solid phase; (iii) solid catalyst with the liquid layer only at the interface with the nanowire (Figure S3b right),[5] where precursor is adsorbed at the solid surfaces and a significant surface diffusion area (including the catalyst, nanowire and even the substrate) accelerate the nanowire growth rate.[6] In the case of a root catalyst growth, the catalyst droplet has a strong interaction with the substrate (catalyst has an obtuse contact angle with the substrate) (**FigureS3c**). The initial precursor decomposition, its dissolution in a liquid catalyst and its diffusion towards the nanowire occur similar to that of the tip catalyst growth case. However, because of the strong interaction, the precipitation fails to raise the catalyst up.[7] In the case of a catalyst-free nanowire growth, a self-catalytic process is believed to take place. By heating the substrate to a temperature above the melting point of a small nanowire nuclear (which have smaller melting point than the bulk due to the high curvature [8-11]), the gaseous precursor react with and dissolve into the liquid. When size of the nuclei exceeds a critical value, it precipitates to form a solid alloy layer beneath the molten curved tip, thus inducing nanowire growth. **Figure S3d** demonstrates the possible correlation between the size of the catalytic particles and the resulting diameters of the nanowires. The minimum radius of the nanowire could be expressed as following [12]:

$$R_m = \frac{2V_1}{RTLn(S)}\sigma_{lv}$$

where V_1 is the molar volume of the droplet, σ_{lv} is the liquid-vapor surface energy, and S is the degree of vapor supersaturation. Accordingly, a smaller catalyst requires a higher degree of supersaturation. Nevertheless, the chemical potential of the component in the metal-alloy catalyst increases as the size of the catalyst decreases due to the Gibbs-Thompson effect:

$$\Delta\mu = \frac{2\gamma}{r}$$

where $\Delta\mu$ is the chemical potential difference of the alloy species in the liquid droplet, γ is the surface energy and r is the radius of curvature of the droplet. Therefore, with the size decreasing, it becomes more difficult to dissolve a vapor component into a liquid alloy, and to reach supersaturation states that induce the growth of nanowires.[12]

In addition to the VLS growth, other growth mechanisms (including such as vapor-solid (VS) and solution–liquid–solid (SLS), where no catalytic liquid metal is needed, and etc.) may take place.[13] For those, we refer the readers to more specialized literature.[14-28]

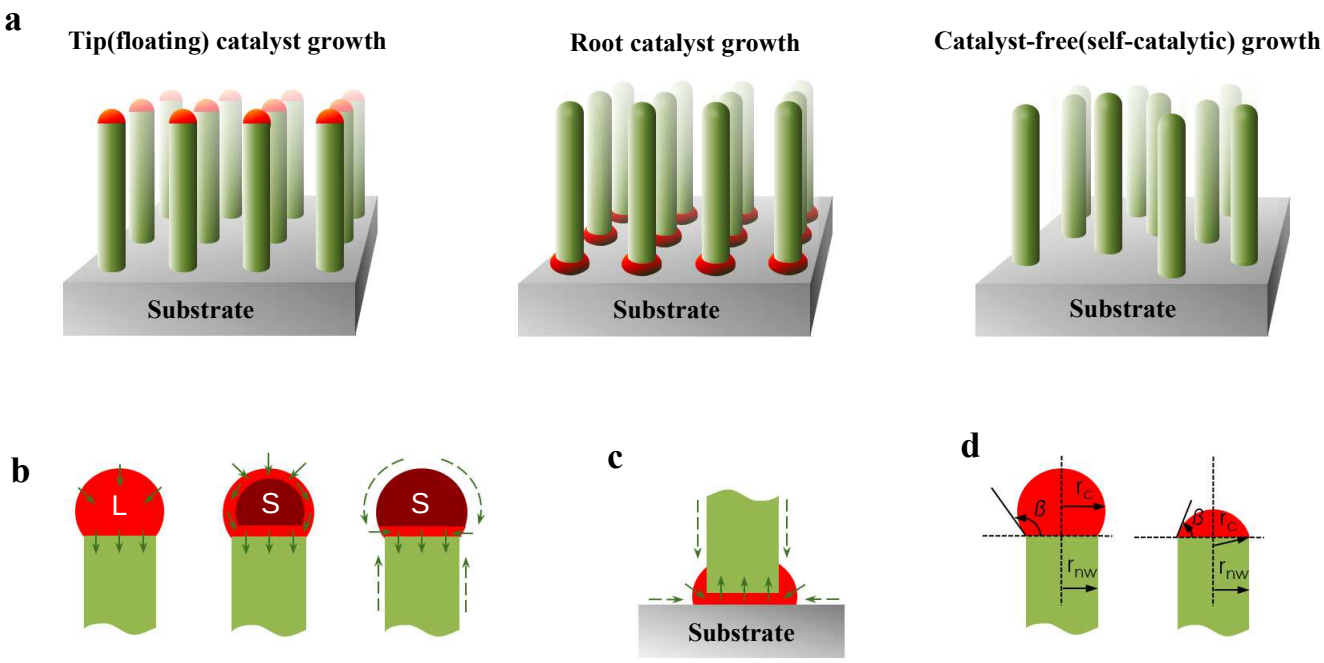

Figure S3. Schematic illustration of nanowires' growth on a substrate by CVD: (a) three common growth types – tip and root catalyst-assisted CVD, catalyst-free CVD; (b) three common types of catalysts at the tip of the nanowires – liquid (L) catalyst, solid (S) catalyst with a liquid surface and interface, solid catalyst with a liquid interface and the corresponding dominating paths for the diffusion of the source atoms; (c) dominating diffusion paths of the source atoms from the root catalyst (liquid phase is shown as an example); (d) relationship between the size of the nanowire and the size and shape of the tip catalyst particle as determined by a balance of the surface tension of the catalyst and the catalyst-nanowire interface tension during the nanowire growth.

Reference

1. X. G. Han, Y. H. Xu, X. Y. Chen, Y. C. Chen, N. Weadock, J. Y. Wan, H. L. Zhu, Y. L. Liu, H. Q. Li, G. Rubloff, C. S. Wang and L. B. Hu, *Nano Energy*, 2013, **2**, 1197-1206.
2. R. S. Wagner and W. C. Ellis, *Appl Phys Lett*, 1964, **4**, 89-90.
3. S. Barth, F. Hernandez-Ramirez, J. D. Holmes and A. Romano-Rodriguez, *Prog Mater Sci*, 2010, **55**, 563-627.
4. H. Y. Wang and G. S. Fischman, *J Appl Phys*, 1994, **76**, 1557-1562.
5. L. E. Jensen, M. T. Bjork, S. Jeppesen, A. I. Persson, B. J. Ohlsson and L. Samuelson, *Nano Lett*, 2004, **4**, 1961-1964.
6. J. Kikkawa, Y. Ohno and S. Takeda, *Appl Phys Lett*, 2005, **86**.
7. Q. Liu, C. Wang, N. Xu and G. Yang, *Phys Rev B*, 2005, **72**, 085417.
8. Z.-Y. Zeng and J.-H. Lin, *RSC Advances*, 2014, **4**, 40251-40258.
9. H. Kim, Y. Son, C. Park, J. Cho and H. C. Choi, *Angew Chem Int Edit*, 2013, **52**, 5997-6001.
10. C. Colombo, D. Spirkoska, M. Frimmer, G. Abstreiter and A. F. I. Morral, *Phys Rev B*, 2008, **77**.
11. W. Lee, M. C. Jeong and J. M. Myoung, *Acta Mater*, 2004, **52**, 3949-3957.
12. M. H. Huang, Y. Y. Wu, H. Feick, N. Tran, E. Weber and P. D. Yang, *Adv Mater*, 2001, **13**, 113-116.
13. K. W. Kolasinski, *Curr Opin Solid State Mater Sci*, 2006, **10**, 182-191.
14. J. S. Lee, S. Brittman, D. Yu and H. Park, *J Am Chem Soc*, 2008, **130**, 6252-6258.
15. Y. Wang, V. Schmidt, S. Senz and U. Gosele, *Nat Nano*, 2006, **1**, 186-189.
16. Y. Baek, Y. Song and K. Yong, *Adv Mater*, 2006, **18**, 3105-3110.
17. C. Y. Wen, M. C. Reuter, J. Tersoff, E. A. Stach and F. M. Ross, *Nano Lett*, 2010, **10**, 514-519.
18. L. C. Campos, M. Tonezzer, A. S. Ferlauto, V. Grillo, R. Magalhaes-Paniago, S. Oliveira, L. O. Ladeira and R. G. Lacerda, *Adv Mater*, 2008, **20**, 1499-1504.
19. J. L. Lensch-Falk, E. R. Hemesath, F. J. Lopez and L. J. Lauhon, *J Am Chem Soc*, 2007, **129**, 10670.
20. S. N. Mohammad, *J Chem Phys*, 2009, **131**.
21. E. Dimakis, J. Lahnemann, U. Jahn, S. Breuer, M. Hilse, L. Geelhaar and H. Riechert, *Cryst Growth Des*, 2011, **11**, 4001-4008.
22. C. Cheze, L. Geelhaar, A. Trampert, O. Brandt and H. Riechert, *Nano Lett*, 2010, **10**, 3426-3431.
23. F. D. Wang, A. G. Dong, J. W. Sun, R. Tang, H. Yu and W. E. Buhro, *Inorg Chem*, 2006, **45**, 7511-7521.
24. L. Ouyang, K. N. Maher, C. L. Yu, J. McCarty and H. Park, *J Am Chem Soc*, 2007, **129**, 133-138.
25. A. G. Dong, F. D. Wang, T. L. Daulton and W. E. Buhro, *Nano Lett*, 2007, **7**, 1308-1313.
26. J. W. Sun, C. Liu and P. D. Yang, *J Am Chem Soc*, 2011, **133**, 19306-19309.
27. Z. Li, O. Kurtulus, N. Fu, Z. Wang, A. Kornowski, U. Pietsch and A. Mews, *Adv Funct Mater*, 2009, **19**, 3650-3661.
28. A. M. Chockla and B. A. Korgel, *J Mater Chem*, 2009, **19**, 996-1001.